Biomech Model Mechanobiol (2013) 12:1115–1125
DOI 10.1007/s10237-012-0467-7

ORIGINAL PAPER

Effects of collagen deposition on passive and active mechanical properties of large pulmonary arteries in hypoxic pulmonary hypertension

Zhijie Wang · Roderic S. Lakes · Jens C. Eickhoff · Naomi C. Chesler

Received: 25 September 2012 / Accepted: 20 December 2012 / Published online: 3 February 2013

Abstract Proximal pulmonary artery (PA) stiffening is a strong predictor of mortality in pulmonary hypertension. Collagen accumulation is mainly responsible for PA stiffening in hypoxia-induced pulmonary hypertension (HPH) in mouse models. We hypothesized that collagen cross-linking and the type I isoform are the main determinants of large PA mechanical changes during HPH, which we tested by exposing mice that resist type I collagen degradation ($Col1a1^{R/R}$) and littermate controls ($Col1a1^{+/+}$) to hypoxia for 10 days with or without β-aminopropionitrile (BAPN) treatment to prevent cross-link formation. Static and dynamic mechanical tests were performed on isolated PAs with smooth muscle cells (SMC) in passive and active states. Percentages of type I and III collagen were quantified by histology; total collagen content and cross-linking were measured biochemically. In the SMC passive state, for both genotypes, hypoxia tended to increase PA stiffness and damping capacity, and BAPN treatment limited these increases. These changes were correlated with collagen cross-linking ($p < 0.05$). In the SMC active state, hypoxia increased PA dynamic stiffness and BAPN had no effect in $Col1a1^{+/+}$ mice ($p < 0.05$). PA stiffness did not change in $Col1a1^{R/R}$ mice. Similarly, damping capacity did not change for either genotype. Type I collagen accumulated more in $Col1a1^{+/+}$ mice, whereas type III collagen increased more in $Col1a1^{R/R}$ mice during HPH. In summary, PA passive mechanical properties (both static and dynamic) are related to collagen cross-linking. Type I collagen turnover is critical to large PA remodeling during HPH when collagen metabolism is not mutated and type III collagen may serve as a reserve.

Keywords Cross-linking · Type I and III collagen · Extralobar pulmonary artery stiffening · Pulmonary hypertension · Viscoelasticity

1 Introduction

Hypoxic pulmonary hypertension (HPH) occurs in patients with lung diseases such as chronic obstructive pulmonary disease (Barbera et al. 2003), cystic fibrosis (Fraser et al. 1999), and sleep apnea (Hiestand and Phillips 2008) and contributes significantly to morbidity and mortality. The devastating consequence of the persistently high arterial blood pressure in the lung is right ventricular (RV) overload and ultimately RV failure. Recently, large conduit pulmonary artery (PA) stiffening has been recognized as a critical factor in pulmonary hypertension (PH) progression that accounts for over a third of the RV workload increase (Stenmark et al. 2006). In clinical studies, an increase in PA stiffness—or a loss of distension during systole—was found to be an excellent predictor of mortality in patients with PH (Mahapatra et al. 2006; Gan et al. 2007). However, the biological determinants of large PA stiffening are not well understood. Moreover, most previous

Z. Wang
Department of Biomedical Engineering, University of Wisconsin at Madison, 2145 ECB; 1550 Engineering Drive, Madison, WI 53706-1609, USA

R. S. Lakes
Department of Engineering Physics, University of Wisconsin at Madison, Madison, WI 53706, USA

J. C. Eickhoff
Biostatistics and Medical Informatics, University of Wisconsin at Madison, Madison, WI 53706, USA

N.C. Chesler (✉)
Department of Biomedical Engineering, University of Wisconsin at Madison, 2146 ECB; 1550 Engineering Drive, Madison, WI 53706-1609, USA
e-mail: chesler@engr.wisc.edu

characterizations of conduit PA mechanical properties were performed statically. As arteries are constantly under pulsatile blood flow and pressure, the dynamic properties, that is, viscoelasticity, may be relevant to ventricular afterload. However, little is known about these changes during PH progression.

Collagen, a major component in the extracellular matrix, accumulates in the PAs markedly in chronic HPH and is a key factor in large PA stiffening (Poiani et al. 1990b; Tozzi et al. 1994; Kobs et al. 2005; Kobs and Chesler 2006; Ooi et al. 2010; Drexler et al. 2008; Wang and Chesler 2011). To further study how collagen accumulation affects arterial stiffening, we have previously examined the differential contributions of collagen content and cross-linking in large PA viscoelastic properties using the combination of a transgenic mouse model (Col1a1), which has a defect in type I collagen degradation, and an anti-fibrotic drug (β-aminopropionitrile, BAPN), which prevents new cross-link formation (Wang and Chesler 2011). With the subsequent decoupling of changes in collagen cross-linking and total content in large, extralobar PAs, we were able to correlate viscoelastic properties with extracellular matrix changes in a smooth muscle cell (SMC) passive state in a normal physiological pressure range of 10–25 mmHg. In the present study, we further investigated both static and dynamic mechanical properties of large PAs during HPH progression in SMC passive and active states in a larger pressure range (10–40 mmHg) that includes pathological elevations in pressure. Moreover, individual contributions of collagen isoforms (type I and III) to PA mechanical properties were examined. We hypothesized that PA mechanical properties are affected by collagen cross-linking and that type I collagen plays a major role in PA remodeling during HPH.

2 Methods

All procedures were approved by the University of Wisconsin–Madison Institutional Animal Care and Use Committee. Breeding pairs of Col1a1^{tmJae} mice on the B6/129 background were obtained from Jackson Laboratory (Bar Harbor, ME). Genotyping by polymerase chain reaction was performed as described previously (Zhao et al. 1999). 16- to 18-week-old Col1a1$^{+/+}$ and Col1a1$^{R/R}$ mice were randomized into three groups: normoxia, 10 days of hypoxia with or without BAPN treatment (Sigma-Aldrich Corp., intraperitoneal injection of 5 mg dissolved in 0.5 ml of PBS, twice per day). During hypoxia, animals were maintained in normobaric hypoxic chamber at controlled O_2 concentration of 10 % with 4 L min^{-1} air flow to maintain the carbon dioxide level at <600 ppm (Ooi et al. 2010). The chambers were opened for less than 30 min at a time for regular animal care or BAPN injections.

Table 1 Experimental groups and animal numbers used in each group

Genotype	Exposure condition/treatment	Set 1	Set 2
Col1a1$^{+/+}$	Normoxia	$N = 6$	$N = 7$
	Hypoxia	$N = 8$	$N = 7$
	Hypoxia + BAPN	$N = 6$	$N = 8$
Col1a1$^{R/R}$	Normoxia	$N = 7$	$N = 7$
	Hypoxia	$N = 6$	$N = 6$
	Hypoxia + BAPN	$N = 6$	$N = 7$

2.1 Vessel harvest and biochemical assays

Mice were euthanized with an overdose pentobarbital sodium ($\sim$ 200 mg/kg) by intraperitoneal injection. Then, a midline sternotomy was performed, and the heart and lungs were removed. Extralobar PAs were excised from the pulmonary trunk to the first branches under microscopy. For the first set of mice (set 1, Table 1), left PAs were mounted in a vessel chamber (Living System Instrumentation (LSI), Burlington, VT) for mechanical testing. After the mechanical tests, PAs were fixed in 10 % formalin for histology. In a separate set of mice with the same experimental exposures (set 2, Table 1), the left and right PAs were harvested, homogenized and the collagen total content and cross-linking were measured biochemically.

2.2 Isolated vessel mechanical tests

In the vessel chamber, PAs were stretched axially 140 %, at the approximate in vivo stretch ratio, to prevent buckling at higher pressures and tested at this fixed length (Kobs et al. 2005; Ooi et al. 2010). Pressure-outer diameter (P-OD) curves were obtained using an isolated vessel mechanical testing system as described previously (Ooi et al. 2010). Physiological saline solution (PSS) was used initially for both perfusate and superfusate to perform vasoactive experiments under cyclic pressures via treatment with a potent vasoconstrictor U46619 (4.5×10^{-7} M, Cayman Chemical, Ann Arbor, MI). Next both perfusate and superfusate were replaced by calcium- and magnesium-free PBS to measure mechanical properties in a SMC passive state under cyclic and static pressure conditions. The perfusate was supplied via a steady flow pump (LSI; Burlington, VT) and an oscillatory flow pump (EnduraTec TestBench; Bose Corporation; Eden Prairie, MN) to achieve static pressurization or cyclic sinusoidal pressurization at 10–40 mmHg at a frequency of 0.01 Hz. Superfusate was continuously circulated and maintained at 37 °C, with pH = 7.4. After each change of fluid medium or between the dynamic and static mechanical tests, the vessels were allowed 30 min to equilibrate, then preconditioned for 10 cycles at 0.014 Hz before data recording as done previously (Kobs et al. 2005). During the dynamic test, P-OD

data were recorded simultaneously by IonWizard software (Version 6.0, IonOptix, Milton, MA) using in-line pressure transducers and amplifiers (PT-F and PM-4, LSI; Burlington, VT) at an acquisition frequency of 1 Hz; and a CCD camera (IonOptix, Milton, MA) connected to an inverted microscope (Olympus, Center Valley, PA) to measure OD at 4× magnification with an acquisition frequency of 1.2 Hz. During the static test, pressure stair steps of 5, 10, 15, 20, 25, 30, 35 and 40 mmHg were applied for 30 s each and P-OD data were recorded as done in the dynamic test. Vessel plastic deformation was checked at a final 5 mmHg step and no plastic deformation was observed.

2.3 Analysis of vessel mechanical properties

The viscoelastic properties of PAs were obtained from pressure-stretch hysteresis as described previously (Wang and Chesler 2011). Briefly, stretch was calculated as the ratio of pressure-dependent OD to OD at the baseline pressures of ~0 or 5 mmHg (OD_0 or OD_5) for dynamic or static mechanical data, respectively. We use OD_5 as reference for static mechanical analysis to permit comparison with previous studies (Kobs et al. 2005; Ooi et al. 2010). PA dynamic stiffness (E) was defined by the slope of the line best-fit to the whole pressure-stretch loop generated by loading and unloading during the 10–40 mmHg cyclic sinusoidal pressurization. The stored energy (W_S) and the dissipated energy (W_D) were defined as the areas of the triangle defined by the maximum and minimum stretch in the hysteresis loop and the area within the hysteresis loop, respectively (Lakes 1999; Mavrilas et al. 2005). Then, damping capacity (D) was calculated as $W_D/(W_D + W_S)$.

To examine the changes in E and D induced by smooth muscle activation, we calculated the differences from the passive state using the following equations:

$$\Delta E(\%) = \frac{E_{\text{active}} - E_{\text{passive}}}{E_{\text{passive}}}$$

$$\Delta D(\%) = \frac{D_{\text{active}} - D_{\text{passive}}}{D_{\text{passive}}}$$

The arteries were assumed to be homogeneous and incompressible. Assuming conservation of mass and no axial extension, the wall thickness (h) as a function of OD, recorded during the 10–40 mmHg cyclic pressurization, was calculated as:

$$h = \frac{1}{2}\left(\text{OD} - \sqrt{\text{OD}^2 - \text{OD}_{40}^2 + (\text{OD}_{40} - 2h_{40})^2}\right)$$

where OD_{40} and h_{40} are the OD and h measured optically (Chesler et al. 2004) at 40 mmHg with the same inverted microscope and CCD camera described above. Then, the local area compliance (C) and circumferential incremental elastic modulus (E_{inc}) were calculated from the P–OD relationship using Hudetz's modification (Hudetz 1979) for an orthotropic vessel having a nonlinear stress–strain relation:

$$C = \frac{\Delta A_i}{\Delta P}$$

$$E_{\text{inc}} = \frac{\Delta P}{\Delta \text{OD}} \cdot \frac{2\text{ID}^2 \times \text{OD}}{\text{OD}^2 - \text{ID}^2} + \frac{2P \times \text{OD}^2}{\text{OD}^2 - \text{ID}^2}$$

where A_i is the inner cross-sectional area and ID is the inner diameter.

2.4 Quantification for collagen subtypes

After mechanical tests, left PAs were saved for histology by fixing in 10 % formalin and preserving in 70 % ethanol. The vessels were then embedded in agar gel, sectioned, and stained with picro-sirius red to identify collagen. Sections were imaged on an inverted microscope (TE-2000; Nikon, Melville, NY) and captured using a Spot camera and software for image capture and analysis (Meta Vue; Optical Analysis Systems, Nashua, NH). Using polarized light, the area positive for collagen isoforms (i.e., type I and type III) was identified by color thresh-holding in the fields of view by a single observer blinded to the experimental condition. Specifically, areas of green (G), orange (O) and yellow (Y) in the cross-section of each vessel ring were measured as area percentage (%) of the total image. Then, percentages of type I and type III collagen were calculated by the combined area of O+Y and the area of G, respectively (Junqueira et al. 1978; Namba et al. 1997).

We previously measured total collagen content (by hydroxyproline, OHP) and cross-linking (by pyridinoline, PYD) biochemically in the same experimental groups using another set of mice (set 2, Table 1) (Wang and Chesler 2011). Because the tissue amount of an individual extralobar PA was too small to obtain an accurate measurement of tissue weight, we kept the harvest procedure consistent for all PAs (from pulmonary trunk to the first branch before entering into the lungs) and present the results as 'μg per vessel' for measured OHP and 'nmol per vessel' for measured PYD. In order to determine the mean content and cross-linking for each collagen subtype, we multiplied the group means of collagen total content (or cross-linking) measured from the biochemistry assays with the group means of the percentage of type I (or type III) collagen measured from histology. The standard deviation of this mean was obtained using the formula presented by Goodman (Goodman 1962).

The mechanical and biological measurements obtained for large PAs for all animals in each experimental group and set are detailed in Table 2.

2.5 Statistics

All results are presented as mean ± SE. For each mouse genotype (mutant or wildtype), comparisons between exposure

Table 2 Mechanical and biological measurements performed on large PAs for each set of animals outlined in Table 1

Set		Mechanical measurements			Histology	Biochemical assays	Measured from combined sets
		Static test (passive)	Dynamic test (passive)	Dynamic test (active)			
1	OD	C	E	E	Type I %		Total Type I
	WT	E_{inc}	D	D	Type III %		Total Type III
2						OHP PYD	

OD outer diameter, *WT* wall thickness, *C* compliance, E_{inc} incremental elastic modulus, *E* dynamic stiffness, *D* damping capacity, *OHP* collagen content, *PYD* cross-linking, *Type I/III* Type I/III collagen

groups were performed by using analysis of variance (ANOVA). Tukey's Honestly Significant Difference (HSD) method was used to control the type I error for the pairwise comparisons between exposure groups. Linear mixed effects model analysis with mouse-specific random effects and an unstructured correlation structure between repeated measures were used to evaluate the pressure-stretch relationship obtained from static mechanical tests. Model assumptions were validated by utilizing residual and normal-probability plots. In order to calculate the standard errors for means of the product between the means of collagen total content (or cross-linking) measured from the biochemical assays and the group means of the percentage of type I (or type III) collagen measured from histology, the nonparametric bootstrap technique with 10,000 replicates was used (Efron and Tibshirani 1993).

The nonparametric Spearman rank correlation test with a permutation analysis (permutation size $M = 10{,}000$) was used to compute the Spearman's correlation coefficient (r_s) and p values for correlations between the averages of passive stiffness (E) or damping capacity (D), and averages of total collagen cross-linking or content for both genotypes combined using SAS version 9.2. To assess linearity, a simple linear correlation coefficient (R^2) was determined for the averages of E or D, and averages of collagen cross-linking or content for both genotypes combined using Microsoft Excel.

Data analysis was conducted using the R software version 2.5.1 (R Foundation for Statistical Computing). All p-values were two-sided and $p < 0.05$ was considered as statistically significant (* vs. normoxia and † vs. hypoxia, $N = 5$–8 per group).

3 Results

3.1 Geometrical and biological changes in large PAs

With HPH, we observed a significant decrease in OD at 40 mmHg when measured in the passive state in both mouse genotypes ($p < 0.05$; Table 3). Inhibition of cross-link formation due to the BAPN treatment did not prevent the reduction in OD in wild-type mice (Col1a1$^{+/+}$), but did in the mutant mice (Col1a1$^{R/R}$). HPH increased PA wall thickness (h) markedly in both mouse types as expected ($p < 0.05$); BAPN treatment prevented this increase, but the effect was only significant in wild-type mice. These changes in h suggest potential differences in collagen deposition between the groups, so next we examined the collagen-relevant biological changes in the large PAs.

As shown in Table 3, HPH increased collagen total content and cross-linking in PAs in both mouse types. As previously reported (Wang and Chesler 2011), BAPN treatment

Table 3 Morphological (*OD* outer diameter, *WT* wall thickness) and biological (*OHP* collagen content and *PYD* cross-linking , percentage of type I and III collagen) parameters measured for large PAs

Genotype	OD at 40 mm Hg (μm)	WT at 40 mmHg (μm)	OD at 5 mmHg (μm)	OHP (μg/vessel)	PYD (nmol/vessel)	Type III collagen (%)	Type I collagen (%)
Col1a1$^{+/+}$							
Normoxia	1189 ± 46	30 ± 3	633 ± 17	0.9 ± 0.1	0.17 ± 0.02	30 ± 3	70 ± 3
Hypoxia	970 ± 46*	47 ± 4*	583 ± 19	1.7 ± 0.1*	0.28 ± 0.03*	24 ± 3	76 ± 3
Hypoxia + BAPN	971 ± 57*	33 ± 3†	553 ± 20*	1.4 ± 0.1*	0.20 ± 0.01†	28 ± 8	72 ± 8
Col1a1$^{R/R}$							
Normoxia	1139 ± 24	30 ± 4	582 ± 15	1.2 ± 0.1	0.17 ± 0.03	20 ± 2	80 ± 2
Hypoxia	992 ± 34*	45 ± 3*	557 ± 12	1.8 ± 0.1	0.25 ± 0.03	44 ± 4*	56 ± 4*
Hypoxia + BAPN	1070 ± 35	38 ± 3	573 ± 17	2.6 ± 0.2*†	0.22 ± 0.02	35 ± 5*	65 ± 5*

Means ± SE are shown. $p < 0.05$, * versus normoxia, † versus hypoxia. $N = 5$–8 per group

prevented the increases in cross-linking in both mouse types, but it had different effects on accumulation; whereas the collagen total content slightly decreased in wild-type mice, it further increased with BAPN treatment in the mutant mice compared to the hypoxia-alone group.

To examine the contributions of individual collagen isoforms in the total collagen accumulation, we quantified the percentages of subtype collagen (Table 3) and found there were no changes in type I and type III collagen percentages in the wild-type mice during HPH or with BAPN treatment. But, interestingly, in the Col1a1$^{R/R}$ mice, hypoxia alone caused an increase in type III collagen percentage ($20 \pm 2\,\%$ in normoxia vs. $44 \pm 4\,\%$ in HPH, $p < 0.05$) and a decrease in type I collagen percentage ($80 \pm 2\,\%$ in normoxia vs. $56 \pm 4\,\%$ in HPH, $p < 0.05$). These changes were not affected by BAPN treatment ($p < 0.05$).

3.2 Differential changes in content and cross-linking of type I and III collagen isoforms

In addition to the relative amount of collagen type I and III (Table 3), we calculated the absolute amount of the content and cross-linking in these collagen isoforms (Fig. 1). We found very different contributions of type I and III collagen to PA total collagen change during HPH between the mouse types: in Col1a1$^{+/+}$ mice, type I but not type III collagen content and cross-linking were significantly elevated after hypoxia; in contrast, in Col1a1$^{R/R}$ mice, type III but not type I collagen significantly increased during hypoxia and formed cross-links.

BAPN had very different effects on PA collagen deposition between the mouse types: in Col1a1$^{+/+}$ mice, BAPN prevented the increases in type I collagen content and cross-linking ($p < 0.05$), and there were no significant changes in type III collagen. In contrast, in Col1a1$^{R/R}$ mice, there were no changes in type I collagen cross-linking with hypoxia alone or combined BAPN treatment despite an increase in total content with BAPN treatment ($p < 0.05$, Fig. 1a); type III collagen total amount and cross-linking both increased significantly after hypoxia and BAPN had minimal effects on these increases ($p < 0.05$, Fig. 1b, d).

3.3 Static mechanical tests suggest passive mechanical properties are dependent on collagen cross-linking in large PAs

To study how deposition of collagen affects PA mechanical properties, we first examined passive mechanical properties in static pressurization conditions. The overall stiffness of the arteries was measured from pressure-stretch (Fig. 2) and stretch-compliance (Fig. 3) relationships. We found in both mouse types that hypoxia increased PA stiffness and BAPN treatment limited this increase. We further examined the material stiffness by calculating incremental elastic modulus (E_{inc}, Fig. 4). Again in both mouse types, hypoxia led to an increase in E_{inc} and BAPN treatment partially prevented

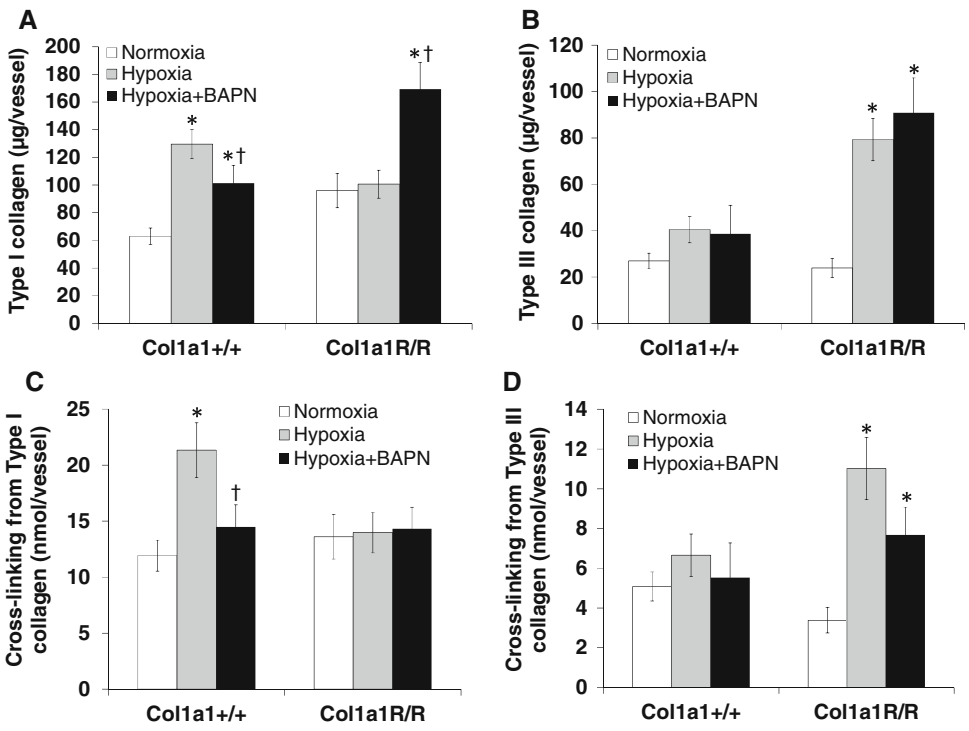

Fig. 1 Type I and type III collagen content and cross-linking in large PAs. $p < 0.05$, * versus normoxia, † versus hypoxia

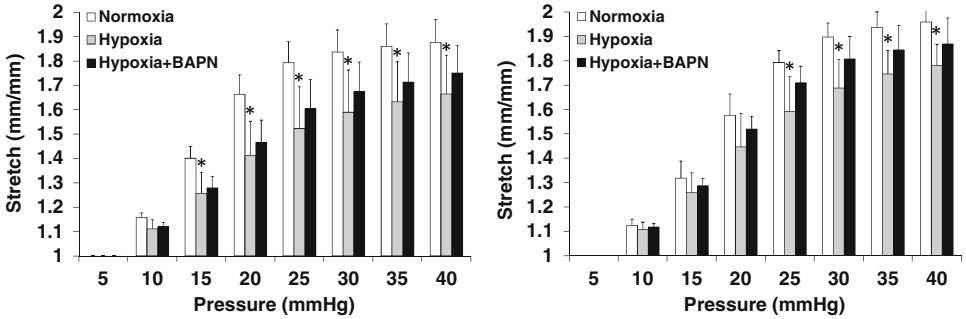

Fig. 2 Pressure-Stretch relationship obtained from static mechanical tests in smooth muscle cell passive state. *Left*: Col1a1$^{+/+}$; *Right*: Col1a1$^{R/R}$. $p < 0.05$, * versus normoxia, † versus hypoxia. $N = 5$–6 per group

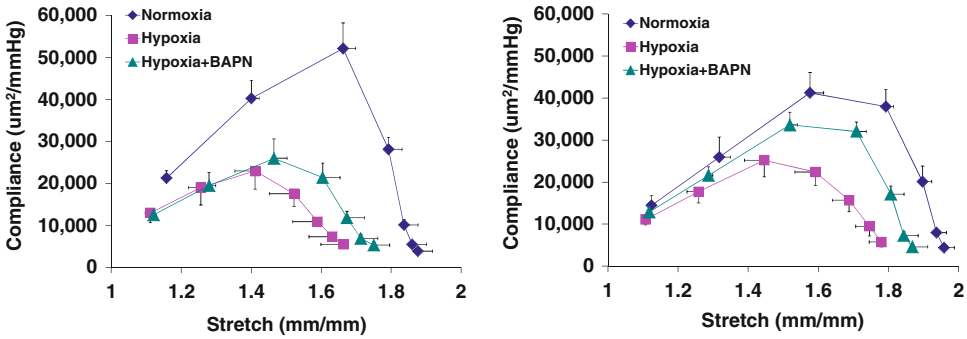

Fig. 3 Compliance of large PAs as a function of stretch measured from static mechanical tests in smooth muscle cell passive state. *Left*: Col1a1$^{+/+}$; *Right*: Col1a1$^{R/R}$. $N = 5$–6 per group

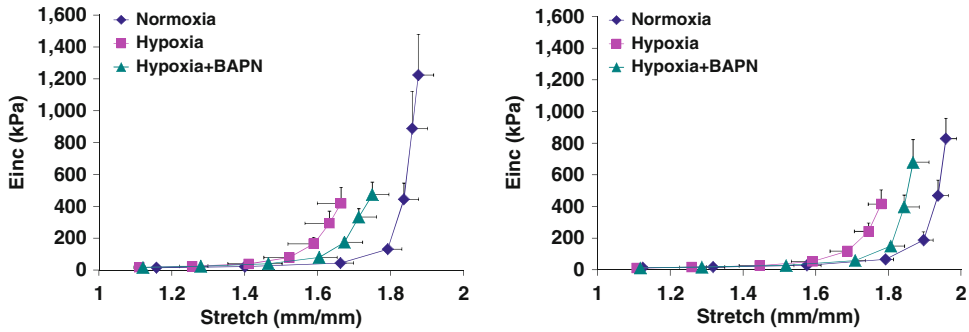

Fig. 4 Incremental elastic modulus (E_{inc}) of large PAs as a function of stretch obtained from static mechanical tests in smooth muscle cell passive state. *Left*: Col1a1$^{+/+}$; *Right*: Col1a1$^{R/R}$. $N = 5$–6 per group

the increase. Therefore, the changes in PA passive stiffness are due in part to changes in collagen cross-linking.

3.4 Dynamic mechanical tests suggest passive viscoelastic properties are dependent on collagen cross-linking in large PAs

Because blood vessels are constantly under pulsatile blood flow and known to be viscoelastic, the dynamic mechanical properties are more physiologically relevant than the static mechanical properties. Thus next we examined the passive viscoelastic properties of PAs using dynamic mechanical tests (Fig. 5a, b). We observed similar trends of changes between Col1a1$^{+/+}$ and Col1a1$^{R/R}$ mice: hypoxia tended to increase E ($p = 0.1$ for Col1a1$^{+/+}$ and $p < 0.05$ for Col1a1$^{R/R}$) and D ($p = 0.2$ for Col1a1$^{+/+}$ and $p = 0.06$ for Col1a1$^{R/R}$), and BAPN treatment prevented these increases. Such preventive effect of BAPN on mechanical property changes due to HPH was similar to that observed from static mechanical tests.

In addition, strong, positive mechanobiological correlations were found between the collagen total cross-linking and E ($R^2 = 0.79$, $r_s = 0.83$, $p < 0.001$; Fig. 5c) as well as D ($R^2 = 0.85$, $r_s = 0.84$, $p < 0.001$; Fig. 5d). In contrast, there were no linear correlations between collagen total content and E ($R^2 = 0.06$) or D ($R^2 = 0.24$). Therefore, our data suggest changes in PA passive mechanical properties (both static and dynamic) are correlated with the changes in collagen cross-linking in both mouse genotypes.

3.5 Dynamic mechanical tests suggest active viscoelastic properties are not linked with measured properties of collagen in large PAs

To comprehensively characterize PA biomechanical changes due to HPH, we also examined the viscoelastic properties

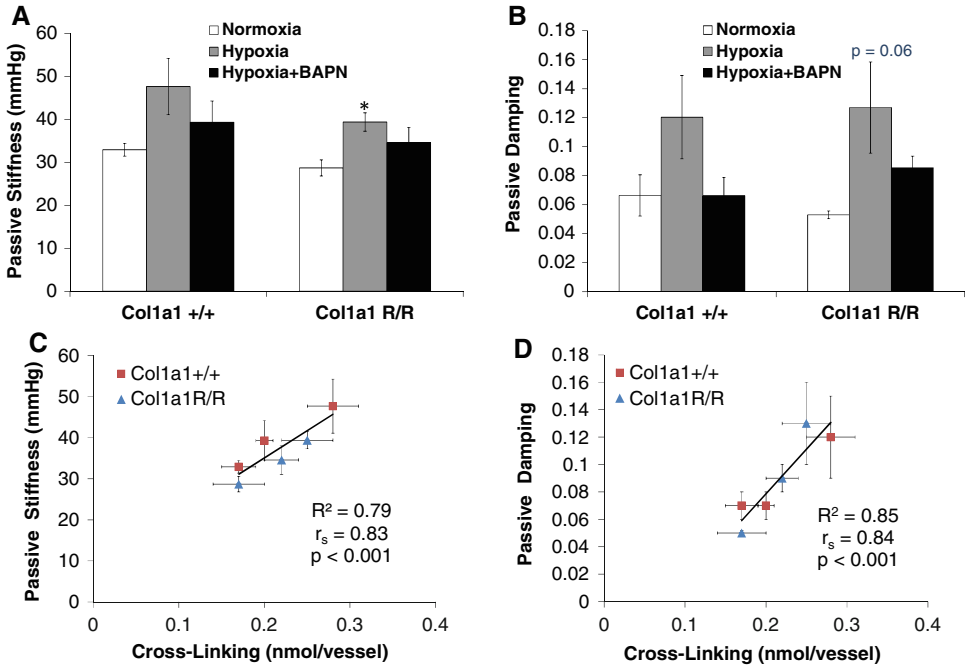

Fig. 5 Stiffness (**a**) and damping capacity (**b**) measured in smooth muscle cell passive state from dynamic mechanical tests. (**c**, **d**) These parameters are correlated with collagen cross-linking of large PAs. $p < 0.05$, * versus normoxia. $N = 5$–8 per group

in the SMC active state after 30 min of incubation with the receptor-independent vasoconstrictor U46619. Overall, the original P–OD curves were leftward-shifted with SMC activation (not shown) in all groups, which is consistent with previous studies (Barra et al. 1993; Santana et al. 2005; Wagner and Humphrey 2011). As shown in Fig. 6a, b, in Col1a1$^{+/+}$ mice, we observed an increase in E (∼142 %, $p < 0.05$ vs. normoxia) with hypoxia and BAPN treatment did not affect the increase (∼137 %, $p < 0.05$ vs. normoxia). In Col1a1$^{R/R}$ mice, we only observed a mild increase in E (∼64 %, $p = 0.16$ vs. normoxia) with hypoxia exposure alone. There were no changes in D between exposures in either mouse type, suggesting a negligible effect of collagen deposition on PA active damping capacity. None of the above changes were associated with collagen total content, cross-linking or subtypes.

3.6 Effects of SMC activation on viscoelastic properties in Col1a1$^{+/+}$ and Col1a1$^{R/R}$ strains

SMC activation induced by U46619 led to a general reduction in E compared to that in the passive state in all groups (normoxia, hypoxia and hypoxia + BAPN), in both mouse types (Fig. 6c). In Col1a1$^{+/+}$ mice, the reduction was less after hypoxia exposure and BAPN treatment did not affect the decreased reduction ($p < 0.05$). In contrast, there were no noticeable differences in the reduction in E in Col1a1$^{R/R}$ mice in the normoxic, hypoxic or hypoxia+BAPN groups.

Not surprisingly, with SMC activation, we observed an increase in D compared to that in the passive state for all groups (normoxia, hypoxia and hypoxia + BAPN) and for both mouse types (Fig. 6d). In Col1a1$^{+/+}$ mice, the increase was less after hypoxia exposure ($p < 0.05$) and BAPN treatment partially prevented the reduced increase. In contrast, in Col1a1$^{R/R}$ mice, there were no significant differences in D in the normoxic, hypoxic or hypoxia + BAPN groups.

4 Discussion

In the present study, we investigated the effects of collagen deposition on passive and active viscoelastic properties as well as static mechanical properties of large PAs in response to HPH. The relevant factors such as collagen total content, cross-linking and isoforms (i.e., type I and type III) and their relationships to PA mechanical properties were examined. We found that collagen cross-linking rather than total amount was correlated with both static and dynamic passive mechanical properties. Moreover, the collagen deposition during HPH was mainly from type I collagen in wild-type (Col1a1$^{+/+}$) mice; but in the mutant (Col1a1$^{R/R}$) mice with type I collagen degradation resistance, collagen deposition was mainly from type III collagen. We did not find a direct linkage between the above biological factors and PA active viscoelastic properties, but different effects of BAPN treatment on wild-type and mutant PA stiffness were observed, which suggests a profound role of collagen deposition in active mechanical properties as will be discussed later.

We have successfully decoupled the changes in collagen content and cross-linking, which otherwise usually change concomitantly, by using the combination of BAPN treatment and a transgenic mouse (Col1a1) with collagen degrada-

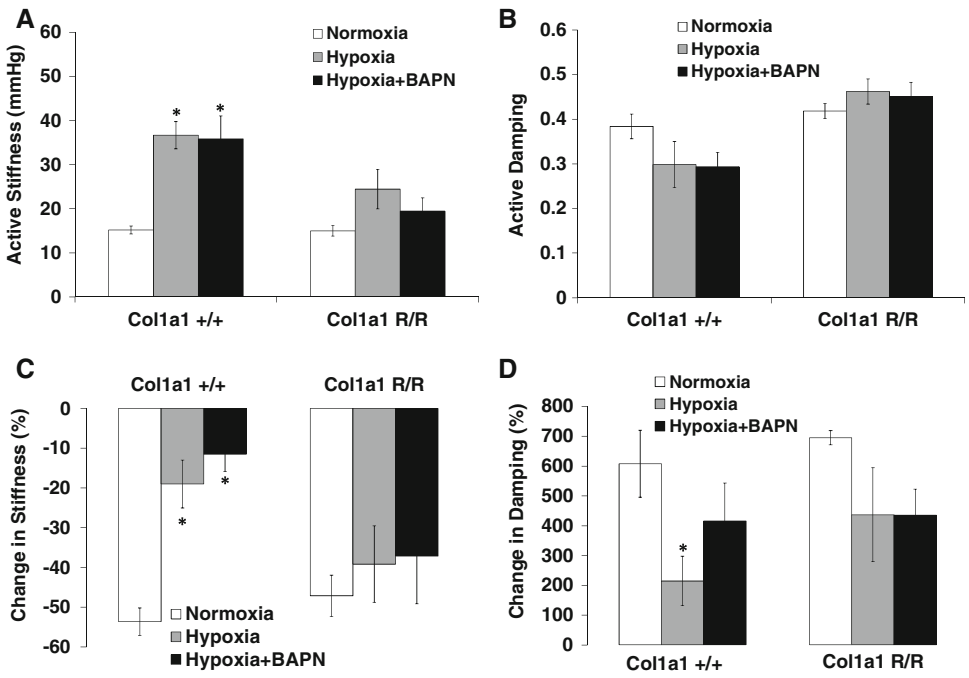

Fig. 6 Stiffness (**a**) and damping capacity (**b**) measured in smooth muscle cell active state from dynamic mechanical tests. Changes in dynamic stiffness and damping capacity from passive to active smooth muscle cell states are shown in (**c**) and (**d**). $p < 0.05$, * versus normoxia. $N = 5$–8 per group

tion resistance in HPH (Wang and Chesler 2011). With such manipulation, we were able to investigate linkages between mechanical properties and biological changes in collagen and found that passive mechanical properties (both static and dynamic) were correlated with collagen cross-linking rather than its total content. This is not surprising because it is anticipated that covalent intercellular and intracellular cross-linking formation in the collagen synthesis confers the mechanical strength to collagen-rich tissues, and numerous studies have demonstrated the contribution of cross-linking to the stiffness of various types of tissue (Berry et al. 1981; Sims et al. 1996; Bruel et al. 1998; Kontadakis et al. 2012; Baker et al. 2012; Carroll et al. 2012). The correlation between damping and cross-linking found in large PAs is novel. It seems to suggest that a source of viscoelasticity may be identified in the properties of covalent bonds.

Our dynamic mechanical tests suggest that PA passive viscoelasticity is correlated with collagen cross-linking. We did not perform the dynamic tests in normal SMC tone, but we expect similar results because we have unpublished experimental results showing similar P–OD curves in the SMC passive and normal states. Similarly, here we did not perform active static tests because our previous studies have shown no significant differences in PA static behavior in SMC active and passive states (Ooi et al. 2010; Tabima and Chesler 2010). Nevertheless, some of our current findings differ from those obtained in our former study (Wang and Chesler 2011): (1) we previously found correlations between changes in collagen total content and PA viscoelasticity; (2) in the Col1a1$^{R/R}$ mice, we previously observed a decrease in D with HPH or BAPN treatment. We attribute these discrepancies to the larger pressure testing range used in the current study: 10–40 mmHg (vs. 10–25 mmHg in the previous work). As the pressure load increases, more collagen fibers will be recruited and the existing cross-linking may be more incorporated into the mechanical load-bearing function. A pressure range of 10–25 mmHg corresponds to the stretch range of 1–1.5, which includes the recruitment of collagen fibers and thus allows us to study the effect of collagen on PA passive mechanical properties (Wang and Chesler 2011). The pressure required for 100 % recruitment of collagen fibers in aorta is 180 mmHg (Armentano et al. 1991), but there is no such result for PAs. Thus, we do not know how many or to what extent collagen fibers were recruited in these stretch ranges. Moreover, it is not clear in the literature at what degree of stretching and/or to what extent collagen cross-links function in providing tissue mechanical strength. Our current data suggest cross-linking may be more critical when the pressure is higher than normal. Because the pressure range in this study better mimics the in vivo situation in HPH (Ooi et al. 2010), we conclude that collagen cross-linking is more critical to PA mechanical properties in the disease state. However, the mechanism by which cross-linking participates in the mechanical loading remains to be elucidated.

More interestingly, by examining the individual contributions of collagen subtypes in the PAs, we found that type I collagen is more responsible for the collagen accumulation in non-mutant mice and thus PA mechanical changes. This finding is novel because type I and type III collagen are major constituents of arterial collagen, but little is known

about individual changes of these isoforms in the remodeling process in response to HPH. In an early study of HPH in rats, the mRNA level of proα1(I) collagen in extralobar PAs was found to peak at 3 days after the onset of hypoxia (Poiani et al. 1990b), suggesting an increase in type I collagen during HPH development; but the type III collagen mRNA was not examined. The ratio of type I to III collagen was quite consistent (2.3:1) between exposures (normoxia, hypoxia or hypoxia+BAPN) in Col1a1$^{+/+}$ mice, which agrees with our previous observation in mouse main PAs (Estrada and Chesler 2009) and other reports on systemic arteries (Halme et al. 1986; Leushner and Haust 1986; Miller et al. 1991). Because of the smaller percentage of type III collagen in PAs, the changes in collagen content and cross-linking with HPH only reached statistical significance for type I collagen in these mice (Fig. 1). In contrast, in Col1a1$^{R/R}$ mice, the ratio of type I to III collagen had a higher baseline (4:1 for normoxia group) compared to the wild-type mice, which is first reported in the present study. Also, the ratio decreased with hypoxia (1.27:1) and BAPN treatment (1.86:1), suggesting an impaired type I collagen accumulation with HPH in the mutant mice. The reduced percentage of type I collagen is likely a direct result of the mutation since matrix degradation can affect the synthesis rate of new fibers. In contrast, type III collagen content and cross-linking increases were pronounced with hypoxia and BAPN treatment in these mice. Therefore, type III collagen seemed to serve as a 'back-up' or 'reserve' for the PA total collagen during remodeling in the mutant mice. Such a compensatory mechanism for arterial remodeling is first reported in this study and warrants further investigation.

SMC activation led to an overall decrease in E and an increase in D compared to the passive state (Fig. 6c, d) as expected based on the prior literature (Boutouyrie et al. 1998; Armentano et al. 2007). The active viscoelastic properties were not correlated with collagen deposition. However, the differences between treatments (normoxia, hypoxia and hypxia + BAPN) and between mouse types suggest collagen deposition may affect SMC function and whole arterial active viscoelasticity. For example, BAPN treatment had different effects on PA active stiffness between mouse types – while the E was elevated ($p < 0.05$) in Col1a1$^{+/+}$ mice, it was at control levels in Col1a1$^{R/R}$ mice. SMC function has been shown to be regulated by ECM proteins (Moiseeva 2001; Stegemann et al. 2005; Hultgardh-Nilsson and Durbeej 2007). Thus, alterations in the SMCs themselves or SMC interactions with ECM components may be responsible for the differences.

Some limitations in the present study are worth noting. First, the dynamic mechanical tests were performed at only one testing frequency (0.01 Hz) in order to compare to our prior experimental findings (Kobs et al. 2005; Ooi et al. 2010; Tabima and Chesler 2010; Wang and Chesler 2011). Future studies will investigate the frequency dependence of PA viscoelasticity. Second, the relative amounts of collagen isoforms (i.e., type I and III) in PAs in the experimental groups were measured from histology because the limited amount of tissue available was not sufficient to perform more accurate protein assays such as ELISA for type I and type III collagen. Sirius red staining has been used as a reliable tool to differentiate collagen subtypes previously (Whittaker et al. 1994; Rich and Whittaker 2005). Other methods such as trichome stains would not be ideal for our collagen detection purpose, especially for thin fibers. Nevertheless, the Sirius red method has some disadvantages. For example, the birefringence of different wall constituents can equal that of the thinnest collagen fibers and complicate the analysis. The frequently crimped collagen fibers make it difficult to ensure the alignment of the fibers does not interfere with the measurement with polarized light, which often leads to underestimation of collagen (Rich and Whittaker 2005). In addition, we assumed the cross-links mostly reside in individual collagen subtypes but neglected the cross-links between collagen subtypes (Henkel and Glanville 1982) or in elastin or other elements of the ECM. The interactions between collagen isoforms may affect collagen biosynthesis, fiber orientation and overall mechanical properties and can be studied in the future. Fourth, the stretch was calculated using an intact diameter (OD_0 or OD_5) as the reference, so residual stretch was not taken into account. We did not measure the residual stress or stretch using the opening angle technique (Fung 1991; Fung and Liu 1991) because it is technically difficult for mouse PA rings. Since it has been shown that the OD of bovine large PAs at a normal diastolic pressure with 1.1 longitudinal stretch is close to the OD obtained using the opening angle technique (diameter ratio $\sim$1) (Tian et al. 2012), we anticipate that our use of an intact diameter as the reference state will not affect our conclusions. Finally, the hemodynamic effects of proximal PA biomechanical changes in HPH were not examined here, but this is of interest because of the prognostic value of proximal PA stiffness in PH. Indeed, understanding the impact of proximal PA stiffening on pulmonary hemodynamics and possibly RV function will assist in understanding the prognostic value of extralobar PA stiffening in PH clinically.

In summary, the present study showed PA passive mechanical properties (both static and dynamic) are related to collagen cross-linking. Large PA stiffening was limited by BAPN treatment, which may partially explain the therapeutic effect of collagen synthesis inhibition as shown in prior studies (Kerr et al. 1984, 1987; Poiani et al. 1990a). Moreover, type I collagen turnover is critical to large PA remodeling due to HPH when collagen metabolism is not mutated and type III collagen may serve as a reserve. This novel finding may provide insights for pulmonary-cardiovascular diseases due to collagen mutations.

Acknowledgments This study is supported by NIH R01 HL086939 (NCC) and AHA Midwest Affiliate Postdoctoral Fellowship 10POST 2640148 (ZW).

References

Armentano RL, Barra JG, Pessana FM, Craiem DO, Graf S, Santana DB, Sanchez RA (2007) Smart smooth muscle spring-dampers. Smooth muscle smart filtering helps to more efficiently protect the arterial wall. IEEE Eng Med Biol Mag 26(1):62–70

Armentano RL, Levenson J, Barra JG, Fischer EI, Breitbart GJ, Pichel RH, Simon A (1991) Assessment of elastin and collagen contribution to aortic elasticity in conscious dogs. Am J Physiol 260(6 Pt 2):H1870–1877

Baker AM, Bird D, Lang G, Cox TR, Erler JT (2012) Lysyl oxidase enzymatic function increases stiffness to drive colorectal cancer progression through FAK. Oncogene. doi:10.1038/onc.2012.202

Barbera JA, Peinado VI, Santos S (2003) Pulmonary hypertension in chronic obstructive pulmonary disease. Eur Respir J 21(5):892–905

Barra JG, Armentano RL, Levenson J, Fischer EI, Pichel RH, Simon A (1993) Assessment of smooth muscle contribution to descending thoracic aortic elastic mechanics in conscious dogs. Circ Res 73(6):1040–1050

Berry CL, Greenwald SE, Menahem N (1981) Effect of beta-aminopropionitrile on the static elastic properties and blood pressure of spontaneously hypertensive rats. Cardiovasc Res 15(7):373–381

Boutouyrie P, Boumaza S, Challande P, Lacolley P, Laurent S (1998) Smooth muscle tone and arterial wall viscosity: an in vivo/in vitro study. Hypertension 32(2):360–364

Bruel A, Ortoft G, Oxlund H (1998) Inhibition of cross-links in collagen is associated with reduced stiffness of the aorta in young rats. Atherosclerosis 140(1):135–145

Carroll CC, Whitt JA, Peterson A, Gump BS, Tedeschi J, Broderick TL (2012) Influence of acetaminophen consumption and exercise on Achilles tendon structural properties in male Wistar rats. Am J Physiol Regul Integr Comp Physiol 302(8):R990–995. doi:10.1152/ajpregu.00659.2011

Chesler NC, Thompson-Figueroa J, Millburne K (2004) Measurements of mouse pulmonary artery biomechanics. J Biomech Eng 126(2):309–314

Drexler ES, Bischoff JE, Slifka AJ, McCowan CN, Quinn TP, Shandas R, Ivy DD, Stenmark KR (2008) Stiffening of the extrapulmonary arteries from rats in chronic hypoxic pulmonary hypertension. J Res Natl Inst Stand Technol 113(4):239–249

Efron B, Tibshirani R (1993) An introduction to the Bootstrap. Chapman & Hall/CRC, Boca Raton

Estrada KD, Chesler NC (2009) Collagen-related gene and protein expression changes in the lung in response to chronic hypoxia. Biomech Model Mechanobiol 8(4):263–272. doi:10.1007/s10237-008-0133-2

Fraser KL, Tullis DE, Sasson Z, Hyland RH, Thornley KS, Hanly PJ (1999) Pulmonary hypertension and cardiac function in adult cystic fibrosis: role of hypoxemia. Chest 115(5):1321–1328

Fung YC (1991) What are the residual stresses doing in our blood vessels? Ann Biomed Eng 19(3):237–249

Fung YC, Liu SQ (1991) Changes of zero-stress state of rat pulmonary arteries in hypoxic hypertension. J Appl Physiol 70(6):2455–2470

Gan CT, Lankhaar JW, Westerhof N, Marcus JT, Becker A, Twisk JW, Boonstra A, Postmus PE, Vonk-Noordegraaf A (2007) Noninvasively assessed pulmonary artery stiffness predicts mortality in pulmonary arterial hypertension. Chest 132(6):1906–1912. doi:10.1378/chest.07-1246

Goodman LA (1962) The variance of the product of K random variables. J Am Stat Assoc 57:54–60

Halme T, Peltonen J, Sims TJ, Vihersaari T, Penttinen R (1986) Collagen in human aorta. Changes in the type III/I ratio and concentration of the reducible crosslink, dehydrohydroxylysinonorleucine in ascending aorta from healthy subjects of different age and patients with annulo-aortic ectasia. Biochim Biophys Acta 881(2):222–228

Henkel W, Glanville RW (1982) Covalent crosslinking between molecules of type I and type III collagen. The involvement of the N-terminal, nonhelical regions of the alpha 1 (I) and alpha 1 (III) chains in the formation of intermolecular crosslinks. Eur J Biochem 122(1):205–213

Hiestand D, Phillips B (2008) The overlap syndrome: chronic obstructive pulmonary disease and obstructive sleep apnea. Crit Care Clin 24(3):551–563, vii. doi:10.1016/j.ccc.2008.02.005

Hudetz AG (1979) Incremental elastic modulus for orthotropic incompressible arteries. J Biomech 12(9):651–655. doi:10.1016/0021-9290(79)90015-0

Hultgardh-Nilsson A, Durbeej M (2007) Role of the extracellular matrix and its receptors in smooth muscle cell function: implications in vascular development and disease. Curr Opin Lipidol 18(5):540–545. doi:10.1097/MOL.0b013e3282ef77e900041433-200710000-00010

Junqueira LC, Cossermelli W, Brentani R (1978) Differential staining of collagens type I, II and III by Sirius Red and polarization microscopy. Arch Histol Jpn 41(3):267–274

Kerr JS, Riley DJ, Frank MM, Trelstad RL, Frankel HM (1984) Reduction of chronic hypoxic pulmonary hypertension in the rat by beta-aminopropionitrile. J Appl Physiol 57(6):1760–1766

Kerr JS, Ruppert CL, Tozzi CA, Neubauer JA, Frankel HM, Yu SY, Riley DJ (1987) Reduction of chronic hypoxic pulmonary hypertension in the rat by an inhibitor of collagen production. Am Rev Respir Dis 135(2):300–306

Kobs RW, Chesler NC (2006) The mechanobiology of pulmonary vascular remodeling in the congenital absence of eNOS. Biomech Model Mechanobiol 5(4):217–225. doi:10.1007/s10237-006-0018-1

Kobs RW, Muvarak NE, Eickhoff JC, Chesler NC (2005) Linked mechanical and biological aspects of remodeling in mouse pulmonary arteries with hypoxia-induced hypertension. Am J Physiol Heart Circ Physiol 288(3):H1209–1217. doi:10.1152/ajpheart.01129.2003

Kontadakis GA, Ginis H, Karyotakis N, Pennos A, Pentari I, Kymionis GD, Pallikaris IG (2012) In vitro effect of corneal collagen cross-linking on corneal hydration properties and stiffness. Graefes Arch Clin Exp Ophthalmol. doi:10.1007/s00417-012-2082-9

Lakes RS (1999) Viscoelastic solids. CRC Press LLC, Boca Raton

Leushner JR, Haust MD (1986) Interstitial collagens in fibrous atherosclerotic lesions of human aorta. Pathol Biol (Paris) 34(1):14–18

Mahapatra S, Nishimura RA, Sorajja P, Cha S, McGoon MD (2006) Relationship of pulmonary arterial capacitance and mortality in idiopathic pulmonary arterial hypertension. J Am Coll Cardiol 47(4):799–803. doi:10.1016/j.jacc.2005.09.054

Mavrilas D, Sinouris EA, Vynios DH, Papageorgakopoulou N (2005) Dynamic mechanical characteristics of intact and structurally modified bovine pericardial tissues. J Biomech 38(4):761–768. doi:10.1016/j.jbiomech.2004.05.019

Miller EJ, Furuto DK, Narkates AJ (1991) Quantitation of type I, III, and V collagens in human tissue samples by high-performance liquid chromatography of selected cyanogen bromide peptides. Anal Biochem 196(1):54–60

Moiseeva EP (2001) Adhesion receptors of vascular smooth muscle cells and their functions. Cardiovasc Res 52(3):372–386

Namba T, Tsutsui H, Tagawa H, Takahashi M, Saito K, Kozai T, Usui M, Imanaka-Yoshida K, Imaizumi T, Takeshita A (1997) Regulation of fibrillar collagen gene expression and protein accumulation in volume-overloaded cardiac hypertrophy. Circulation 95(10):2448–2454

Ooi CY, Wang Z, Tabima DM, Eickhoff JC, Chesler NC (2010) The role of collagen in extralobar pulmonary artery stiffening in response to hypoxia-induced pulmonary hypertension. Am J Physiol Heart Circ Physiol 299(6):H1823–1831. doi:10.1152/ajpheart.00493.2009

Poiani GJ, Tozzi CA, Choe JK, Yohn SE, Riley DJ (1990a) An antifibrotic agent reduces blood pressure in established pulmonary hypertension in the rat. J Appl Physiol 68(4):1542–1547

Poiani GJ, Tozzi CA, Yohn SE, Pierce RA, Belsky SA, Berg RA, Yu SY, Deak SB, Riley DJ (1990b) Collagen and elastin metabolism in hypertensive pulmonary arteries of rats. Circ Res 66(4):968–978

Rich L, Whittaker P (2005) Collagen and picrosirius red staining: a polarized light assessment of fibrillar hue and spatial distribution. Braz J Morphol Sci 22(2):97–104

Santana DB, Barra JG, Grignola JC, Gines FF, Armentano RL (2005) Pulmonary artery smooth muscle activation attenuates arterial dysfunction during acute pulmonary hypertension. J Appl Physiol 98(2):605–613. doi:10.1152/japplphysiol.00361.2004

Sims TJ, Rasmussen LM, Oxlund H, Bailey AJ (1996) The role of glycation cross-links in diabetic vascular stiffening. Diabetologia 39(8):946–951

Stegemann JP, Hong H, Nerem RM (2005) Mechanical, biochemical, and extracellular matrix effects on vascular smooth muscle cell phenotype. J Appl Physiol 98(6):2321–2327. doi:10.1152/japplphysiol.01114.2004

Stenmark KR, Fagan KA, Frid MG (2006) Hypoxia-induced pulmonary vascular remodeling: cellular and molecular mechanisms. Circ Res 99(7):675–691. doi:10.1161/01.RES.0000243584.45145.3f

Tabima DM, Chesler NC (2010) The effects of vasoactivity and hypoxic pulmonary hypertension on extralobar pulmonary artery biomechanics. J Biomech 43(10):1864–1869. doi:10.1016/j.jbiomech.2010.03.033

Tian L, Lammers SR, Kao PH, Albietz JA, Stenmark KR, Qi HJ, Shandas R, Hunter KS (2012) Impact of residual stretch and remodeling on collagen engagement in healthy and pulmonary hypertensive calf pulmonary arteries at physiological pressures. Ann Biomed Eng 40(7):1419–1433. doi:10.1007/s10439-012-0509-4

Tozzi CA, Christiansen DL, Poiani GJ, Riley DJ (1994) Excess collagen in hypertensive pulmonary arteries decreases vascular distensibility. Am J Respir Crit Care Med 149(5):1317–1326

Wagner HP, Humphrey JD (2011) Differential passive and active biaxial mechanical behaviors of muscular and elastic arteries: basilar versus common carotid. J Biomech Eng 133(5):051009. doi:10.1115/1.4003873

Wang Z, Chesler NC (2011) Role of collagen content and cross-linking in large pulmonary arterial stiffening after chronic hypoxia. Biomech Model Mechanobiol 11(1–2):279–289. doi:10.1007/s10237-011-0309-z

Whittaker P, Kloner RA, Boughner DR, Pickering JG (1994) Quantitative assessment of myocardial collagen with picrosirius red staining and circularly polarized light. Basic Res Cardiol 89(5):397–410

Zhao W, Byrne MH, Boyce BF, Krane SM (1999) Bone resorption induced by parathyroid hormone is strikingly diminished in collagenase-resistant mutant mice. J Clin Invest 103(4):517–524. doi:10.1172/JCI5481